ULTRAVIOLET PHOTOMETRY OF THE ECLIPSING VARIABLE CW CEPHEI

Stanley Sobieski
National Aeronautics and Space Administration
Goddard Space Flight Center
Greenbelt, Maryland

ABSTRACT

An extended series of photometric observations were made of the eclipsing variable CW Cephei using the Wisconsin instrument on OAO-2. Approximate elements which were derived based solely on the eclipse depths and shape of the secondary are in satisfactory agreement with those found using ground-based observations. However, persistent asymmetries and anomalous light variations, all larger than the expected experimental error, were also found; subsequent ground-based observations show H_α entirely in emission indicating the presence of an extended gaseous system surrounding one or both of the components. Consistent solutions utilizing all data at all wavelengths were not found.

In addition to the light curve analysis, a detailed comparison was made of the flux distribution of the binary relative to that for the nominally unreddened stars δ Pic B1 III and η Aur B3 V to investigate the effects of interstellar extinction. The observations for these comparison stars were obtained near to the time of the binary observations, thereby minimizing spurious results due to instrumental changes. The resultant extinction curves, normalized at 3330 Å, show a relatively smooth increase with decreasing wavelength; no conspicuous hump near 2200 Å is evident. Additionally assuming E(B-V) = 0.68 a smaller amplitude for the curves is found than that for the Perseus region given by Stecher.

I. INTRODUCTION

Starting in mid-April, 1971 the OAO-2 spacecraft began to be stable for extended observing periods while pointed toward the region around Cepheus, and it became feasible to obtain complete ultraviolet light curves of the eclipsing binary CW Cephei. Petrie's (1947) observations of CW Cephei show it to be a double line spectroscopic binary consisting of two early B stars of nearly equal mass but with a differential spectroscopic luminosity $\Delta m = 0.30 \pm 0.03$. It is designated as No. 69 (bright) by Blaauw, Hiltner and Johnson (1959) in their photometric study of the Cep OB 3 association. They list for it B-V = 0.41 and U-B = -0.52; the application of the Q-method results in unreddened colors of $(B-V)_o = -0.27$, $(U-V)_o = -1.04$, and hence a color excess E(B-V) = 0.68. Its revised MK classification is B1.5 Vn according to Garrison (1970), while the intermediate band and β index photometry of Crawford and Barnes (1970) and that of McNamara (1966) leads to a somewhat earlier classification. These later classifications and that based on the earlier photometry are in substantial agreement. Membership in the association appears certain, based on the binary's location in the color-magnitude plane after corrections are made for interstellar absorption using R = 3.0. By implication then, one can expect that the binary is young, i.e. of the order of the expansion age of the association, which is given by de Vegt (1966) to be approximately 1.6×10^6 years. Abrami and Cester (1960) obtained approximate orbital solutions from two color photoelectric light curves. They found that primary eclipse is a partial transit and they confirmed that the components, though quite similar in surface brightness, are distinctly different in size. A complete rediscussion of this system is being prepared by Il-Seong Nha (1971) based on his new multi-color photoelectric observations. Of some interest is his report of finding rapid apsidal motion.

II. DATA REDUCTION

The present observations were made with the four photometers in the University of Wisconsin instrumentation on OAO-2. A total of 49 data points, each being the mean of six separate measurements of the binary, were obtained over 29 orbits. Dark and calibration readings were obtained at least once per orbit for each photometer. In addition, 6 orbits were dedicated to sky measurements distributed over the nine days of observing. The majority of the orbits between #12280 and #12411 were used for this program. The 10 arc-min field aperture was decentered from the nominal position of the binary by 25 arc min in order to avoid photometric contamination by a nearby fainter B star; sky readings were taken 30 arc min north of this nominal pointing. No attempt was made to obtain data with the shortest wavelength filter and all data from the longest wavelength filter were rejected due to contamination by the unavoidable inclusion of a faint late-type star in the aperture. The other short wavelength data appear to be free of this contamination since the eclipse depths appear to be normal. All data were reduced in the manner suggested by Code (1970). The flux measured through filter "i" with photometer "j" relative to that at λ_{eff} = 3330 Å is given by

$$\log \frac{F_i}{F_{3330}} = \log \left[\frac{(\text{Star}_i - \text{Dark}_j) - (\text{Sky}_i - \text{Dark}_j)}{\text{Calibration}_j - \text{Dark}_j}\right] - \log \left[\frac{(\text{Star}_1 - \text{Dark}_1) - (\text{Sky}_1 - \text{Dark}_1)}{\text{Calibration}_1 - \text{Dark}_1}\right] + \log \Delta_i$$

The correction factors Δ_i are those suggested by Code but as amended by Holm (1971) to allow for the declining sensitivity of photometer #4. Linear interpolation between dark measures gave the dark appropriate at the time of the star or sky measurement. The means for all calibration measurements obtained during the experiment were used to normalize the data from each photometer. Heliocentric orbital phases corresponding to the mean GMT of each observation were computed using Nha's (1971) ephemeris, kindly supplied prior to publication,

$$\text{JD} = 2435373.4487 + 2^{d}.72919396E \pm 0^{d}.0256 \sin (0.07018E - 31^{\circ}.55)$$

where E = 2083 for the observed primary minimum. Approximate times of minima were determined graphically from the data, and they are in excellent agreement with this ephemeris. The observed epochs for primary and secondary eclipses are JD 2441058.270 and JD 2441054.128, respectively.

III. INTERSTELLAR EXTINCTION

In order to investigate the ultraviolet extinction of CW Cep, relative fluxes were found first by forming the means of data taken on April 10 and April 15, 1971 when the system was at maximum light. The approximate effective wavelengths corresponding to each flux measurement, the data for CW Cep expressed in magnitudes, and similar data for two nominally unreddened stars are presented in the first four columns of Table 1. The original data for the two comparison stars were very kindly supplied by the University of Wisconsin, and they were reduced in the same manner as is described above. The stars η Aur, B3 V, and δ Pic, B1.5, were selected to match,

Table 1. Observational Data

	Relative Flux (mag)			Extinction			
λ (1)	CW Cep (2)	δPic (3)	ηAur (4)	CW-δPic (5)	CW-ηAur (6)	Bless, Savage (7)	Stecher (8)
3330	0.00	0.00	0.00	0.00	0.00	0.00	0.00
2980	-0.03	-0.46	-0.36	0.63	0.49	0.65	0.8
2940	0.06	-0.12	-0.34	0.26	0.59	0.85	1.0
2460	0.43	-1.16	-0.80	2.34	1.81	2.34	3.0
2380	0.59	-0.96	-1.04	2.27	2.39	2.90	3.4
2040	0.40	-1.26	-1.47	2.44	2.75	4.00	5.5
1920	0.14	-1.93	-1.55	3.05	2.48	3.32	5.2
1680	-0.02	-2.14	-1.68	3.11	2.44	2.48	3.8
1500	-0.83	-2.60	-2.19	2.59	2.00	2.58	4.3
1380	-1.29	-2.75	-2.19	2.14	1.32	3.07	5.2

respectively, the original and the more recent spectral classifications of CW Cep. Just as important, these observations were obtained at approximately contemporaneous epochs, thus minimizing any effects of instrumental variation. The extinction law is defined here as the difference in magnitude at each effective wavelength between the binary and comparison star, normalized to unity color excess. It differs somewhat from the usual representation in that Δ_m is set equal to zero, arbitrarily, at λ = 3330 Å. The differential magnitudes thus formed are listed separately in columns 5 and 6 of Table 1 while the "average" extinction curve found by Bless and Savage (1972) from OAO-2 observations and that found for the Perseus region by Stecher (1969) are given in the last two columns. The data and the two reference extinction curves are shown in Figure 1. It is immediately evident by intercomparing these curves that the shape of the extinction curve for CW Cep differs markedly from that appropriate to the Perseus region. It is also seen that the average extinction fits the observed data only poorly. Most conspicuous is the apparent absence of the $4.6\mu^{-1}$ bump and the turning-down of the curve at the shortest wavelengths. The overall shape resembles that found by Bless and Savage for $\theta^1 + \theta^2$ Ori except that the amplitude, i.e. relative absorption, is greater for CW Cep in the mid-ultraviolet range. No definite explanation can be offered for the unusual shape of this extinction curve. The fact that the photometric colors are consistent with the spectral type, and that the resultant position of the binary in the color-magnitude diagram of the association appears reasonable after the visible wavelength data are corrected for reddening and absorption with the usual relations, suggests that the absorbing medium is normal, at least in regard to its properties at visible wavelengths. In support of this view, spectra of CW Cep, obtained with the GSFC Cassegrain spectrograph and 36-inch telescope, show moderately strong 4430 Å absorption; the estimated equivalent width of 2-3 Å appears consistent with the E(B-V) = 0.68. On the other hand these same spectra show H_α entirely in emission confirming the report of Wackerling (1970). Its strength appears to vary from approximately 3 to 5 Å as a function of the orbital phase. With this evidence for the presence of an extended gaseous system about one or both components one can speculate that the intrinsic flux distribution is abnormal in the sense that overlying Balmer emission could be modifying the observed ultraviolet flux distribution in a way similar to that found for Be stars. However, the net effect of this would be to exaggerate the apparent absorption at the shortest wavelengths where the Balmer emission would be the weakest which, of course, is contrary to what is observed. Furthermore, this emission as opposed to strategically located line emission cannot explain the absence of the

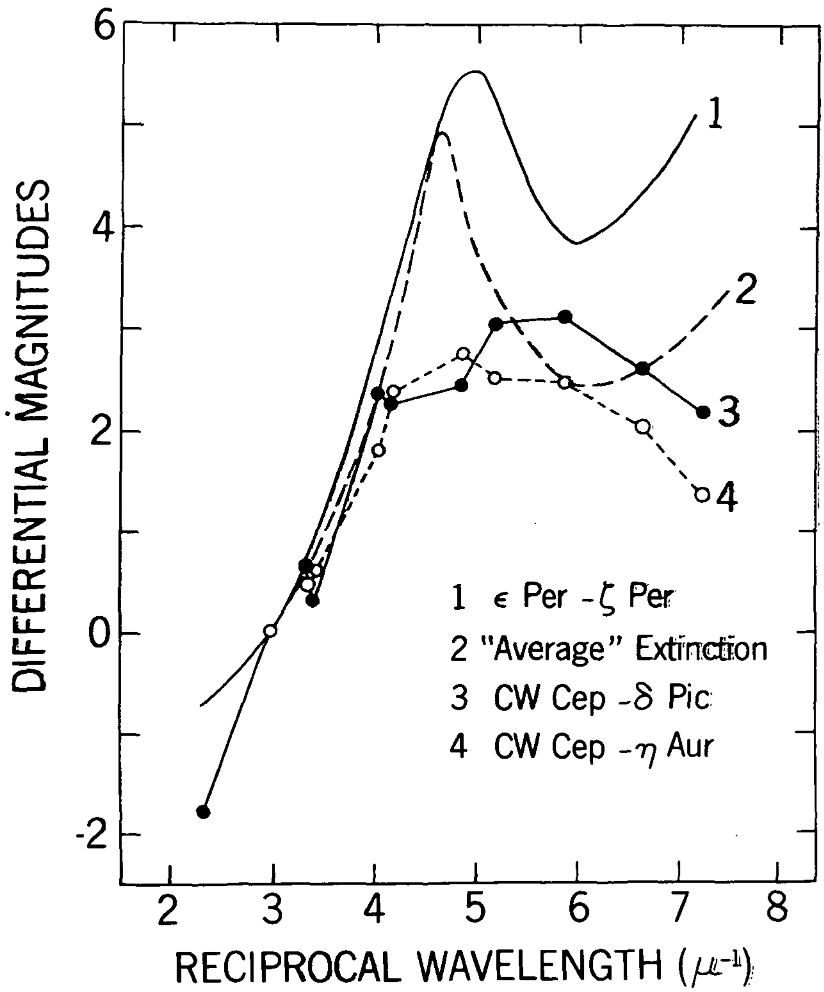

Figure 1.—Ultraviolet extinction curves for CW Cep formed with (1) δ Pic and (2) η Aur, as comparison stars. Curves labelled (3) and (4) refer respectively to the average extinction given by Bless and Savage (1972) and to the extinction in Perseus according to Stecher (1969).

$4.6\mu^{-1}$ bump. It should be noted that spectral scans of θ^1 + θ^2 Ori had not revealed emission at $4.6\mu^{-1}$. It is likely that for CW Cep both conditions obtain, i.e., the ultraviolet flux distribution may well be abnormal, and the interstellar medium or perhaps the immediate stellar environs may be peculiar. Like θ^1 + θ^2 Ori, CW Cep is a multiple system and, additionally, is a member of a young association. It would be of interest to determine if the infrared color excess is unusual as is reported for θ^1 + θ^2 Ori. Of course, data for other members of the Cep OB 3 association would be valuable in elucidating this puzzle.

IV. LIGHT CURVE ANALYSIS

The original objective was to verify the theoretical limb-darkening coefficients by solving the light curves. This could not be done due to instrumental problems which resulted in incomplete coverage and poor phase resolution. Hence, only approximate solutions were possible. Pre-primary maximum is adequately observed as is the entire secondary eclipse, but the egress of primary eclipse is represented by few observations of low weight, and the post-primary maximum is essentially unobserved. Comparison stars were not used as controls, but no systematic differences in light levels were detected for the phases in the pre-primary maximum for which redundant data were available and also for the shallow partial phases of primary ingress.

The light curves, consisting of the highest weight data corresponding to the largest signal to noise cases, are shown in Figure 2 where for simplicity the individual data points have been connected by straight lines. On the basis of visual inspection of the data, rectification in the main appeared unwarranted although some curvature in the maximum of the 1920 Å light curve seems to be present.* The proximity effects, if present, are small but peculiar light variations are evident at the shoulders of both eclipses. Primary eclipse is grossly asymmetric but it must be recalled that egress is only poorly represented. Secondary eclipse changes shape with wavelength. To quantify the shapes of both eclipses, the shape parameter $\chi(n = 0.8)$, as defined by Russell and Merrill (1952) was determined from smooth curves passed through the data for the ingress of primary and the combined data from both branches of secondary. The shape parameters, the observed eclipse depths, and their mean values which are used in a nomographic solution are listed in Table 2. All observational data are tabulated in Appendix I. Because of the paucity of data and the peculiar light variation at the shoulders an uncertainty in the unit light level existed at several wavelengths for data taken during the eclipses. The values of the corrections listed in Table 2, which were applied to all eclipse data, are those which force the light curve to attain unit light near to external tangency. The correction in magnitudes was subtracted from each data point before the corresponding shape parameter was calculated.

The variation in the χ's for secondary eclipse is quite

*One can show that, based on the solution given later in this paper, the effects of reflection and photometric ellipticity should be observed, and one must conclude that the scatter in the present data masks these effects.

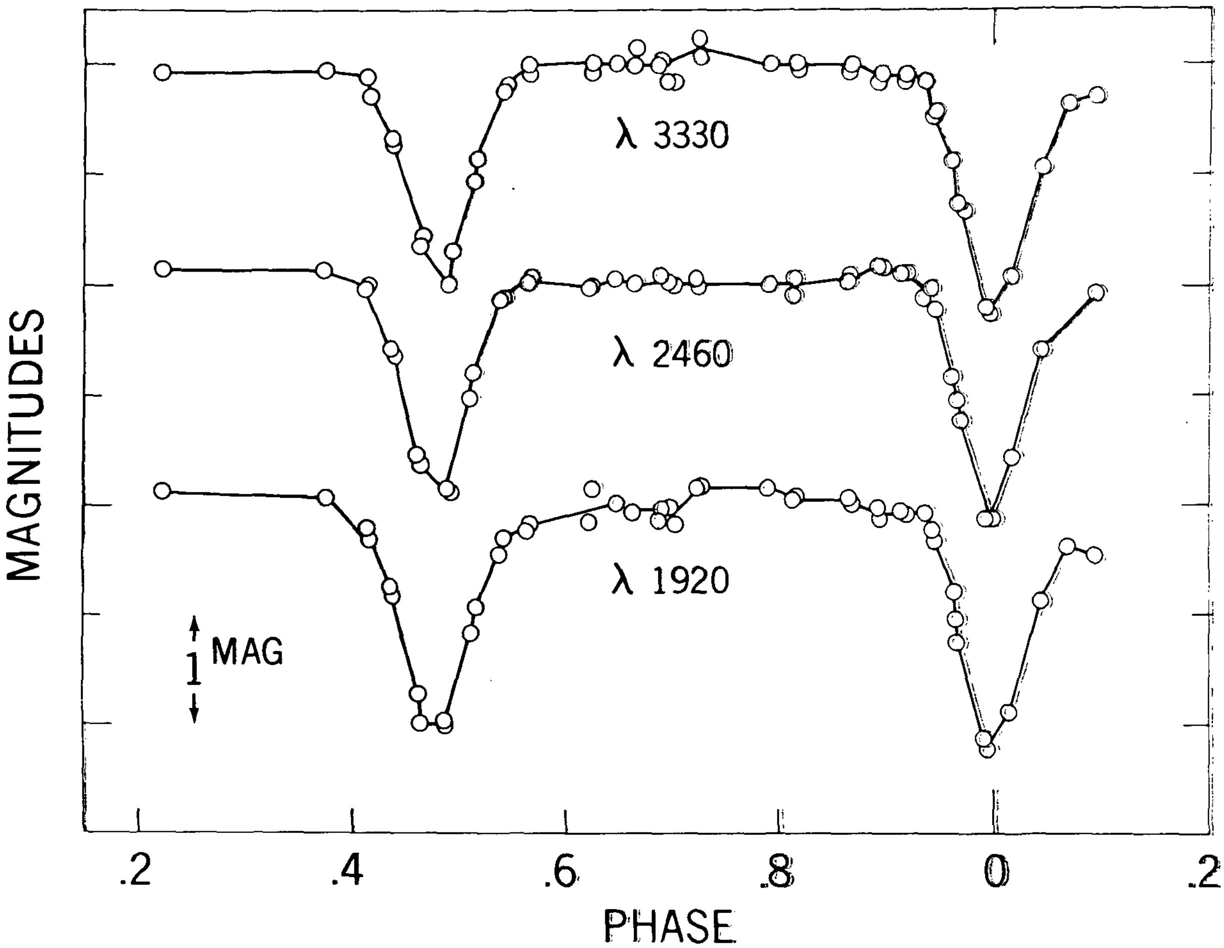

Figure 2.—Representative light curves of CW Cep.

large; the sense of the variation is that the branches steepen with decreasing wavelength. Even if one excludes the case where the corrections were applied, the variation is much larger than can be explained by changing the limb darkening of the eclipsed secondary components.* On the other hand, both the eclipse depths and the shape of primary remain constant. The depths of the eclipses are similar to those found by Abrami and Cester, $\Delta m_{prim} = 0.44$ and $\Delta m_{sec} = 0.37$. This implies that, to a first approximation, the surface brightnesses of the components are alike.

* Although the run of the eclipse is only poorly defined, the data at minimum for the 1920 Å light curve suggest that a total phase may exist.

Table 2. Computed Parameters

	3330 Å			2460 Å		1920 Å		
Eclipse	Pri I	Pri II	Sec	Pri	Sec	Pri	Sec I	Sec II
Depth (mag)	0.473	0.455	0.380	0.454	0.377	0.451	0.395	0.360
Shape $\chi(n=0.8)$	0.274	0.273	0.315	0.251	0.353	0.249	0.398	0.440
Correction (mag)	0	0.025	0	0	0	0	0	0.04

In attempting a nomographic solution, it was found that the depths and line shape relation for primary eclipse yielded no solution at any wavelength, while the secondary eclipse shapes all yielded solutions specifying primary eclipse to be a geometrically deep partial transit. The nomographic solution based on the mean depths and shape of secondary yielded the following elements: ratio of radii = 0.69, radius of primary = 0.26, orbital inclination = 83° and the luminosity of the primary = 0.7. The usual normalizations were adopted, the ratio of surface brightness was set equal to 0.9 (the value used by Abrami and Cester), and a limb darkening of 0.6 was assumed for both components. These elements agree in the main with those found by Abrami and Cester and, in view of the low precision and scarcity of the data, further refinement is considered unwarranted. The computed solutions of Abrami and Cester and that given here during the minima are shown along with the 2460 Å data in Figure 3.

V. DISCUSSION

The system of CW Cep is unusual in many respects. To recapitulate, the ultraviolet extinction is abnormal, emission in H_α is observed, peculiar light variations appear at the shoulders of the minima, and the shape of secondary eclipse varies with wavelength in the ultraviolet. The photometric solution implies an approximate difference in luminosity of $\Delta m = 0.9$, which is inconsistent with that determined spectroscopically. Both components should be well situated on the main sequence if the expansion age of the association applies, since the contraction to the main sequence is given by Iben (1965) for comparable mass stars as 1.5×10^5 years while the main sequence life time is of the order of 10^7 years. And yet from the ratio of the radii or the differential luminosity, either the primary has evolved away from the main sequence or the secondary is a subdwarf. On the basis of the empirical mass-radius relation given by Harris, Strand and Worley (1963), Petrie's spectroscopic solution combined with the photometric results would indicate that the primary is evolved. These questions and particularly the problem of the variation of the eclipse shapes cannot be resolved solely with the present photometric data. If an extended atmosphere exists about either one of the components then one may question the applicability of the Russell-Merrill model and the elements derived thereby. It is easy to show that for a system undergoing eclipses where the geometric depth $p_o = -1.0$, i.e. the case of internally tangent eclipses, a large change can be induced in the shape parameter by moderate changes in the radii. For example, a 10% change in the radius of the secondary star in CW Cep could account for the observed χ variation if the radius decreases

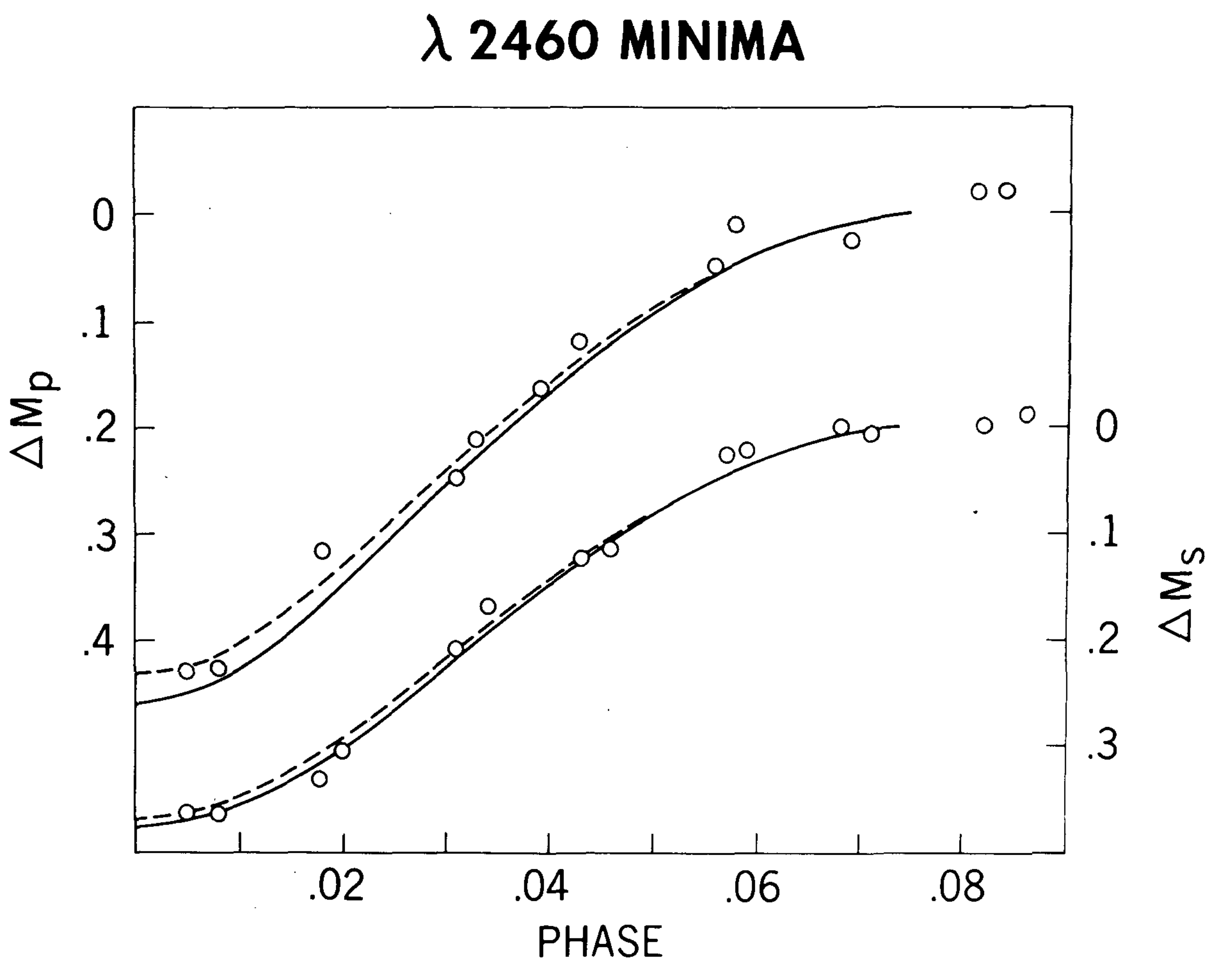

Figure 3.—Computed solutions of Abrami and Cester (1960), represented by the dotted curve, and the present work, given by the solid curve, are shown with the 2460 Å data.

with decreasing wavelength. This situation could obtain if the smaller secondary were surrounded by an optically thin shell which emits a Balmer continuum. An optically thick shell surrounding the larger (and presumably more evolved) star would produce the inverse effect.* Unfortunately this picture of the binary aggravates the already unusual ultraviolet extinction by requiring the true extinction freed of the anomalous shell flux to turn down even more steeply at the shortest wavelengths. Additional observations, particularly

* The phase of external tangency should vary but the photometric difficulties at the shoulders will mask this effect.

scanner measures of the flux distribution, may resolve some of these problems.

I would like to express my appreciation to Dr. Code for making available the large amount of observing time necessary to carry out this research. My thanks also go to Drs. M. Molnar and A. Holm, University of Wisconsin, and to Drs. S. Heap, D. Leckrone and D. West at GSFC for their assistance in preparing the program and for the many useful discussions afterwards.

REFERENCES

Abrami, A. and Cester, B. 1960, Osserv. Astron. Publ. Trieste, No. 300.
Blaauw, A., Hiltner, W. A. and Johnson, H. L. 1959, Ap. J. 130, 69.
Bless, R. C. and Savage, B. D. 1972, this volume.
Code, A. D. 1971, private communication.
Crawford, D. L. and Barnes, J. V. 1970, Astr. J. 75, 952.
De Vegt, Chr. 1966, Zeit. F. Astrop. 64, 268.
Garrison, R. F. 1970, Astr. J. 75, 1001.
Harris, D. L., Strand, K. Aa. and Worley, C. E. 1963, in Basic Astronomical Data, ed. K. Aa. Strand (Chicago: University of Chicago Press), p. 273.
Holm, A. V. 1971, private communication.
Iben, I. 1965, Ap. J. 141, 421.
McNamara, D. H. 1966, in Spectral Classification and Multi-colour Photometry, I.A.U. Symp. No. 24, eds. K. Loden, L. D. Loden and U. Sinnerstad (New York: Academic Press) p. 190.
Nha, Il-Seong 1971, unpublished doctoral thesis, University of Pennsylvania.
Petrie, R. M. 1947, Publ. Dominion Astrop. Obs. 7, 305.
Russell, H. N. and Merrill, J. E. 1952, Contr. Princeton No. 26.
Stecher, T. P. 1969, Ap. J. 157, L125.
Wackerling, L. R. 1970, Mem. Roy. Astron. Soc. 73, 153.

Appendix I. Observed Data for CW Cep

Phase	m_λ			
	λ 3330 Å	2980 Å	2460 Å	1920 Å
0.018	0.384	0.349	0.316	0.372
043	191	152	120	167
069	076	070	---	064
094	060	---	019	079
223	016	012	-033	-028
375	010	018	-031	-011
412	020	-012	007	040
415	057	---	000	065
437	133	080	114	147
440	142	122	123	168
463	328	285	306	346
466	305	331	333	401
488	399	350	364	389
491	337	339	366	400
514	210	228	208	237
517	164	173	158	190
539	047	023	026	088
542	037	036	022	060
565	-002	019	-002	047
568	021	031	-014	039
621	-002	-010	005	027
624	014	011	006	027
648	-000	-006	-011	000
662	004	-034	000	018
663	-033	---	004	---
687	003	-014	---	029
689	-010	014	-016	007
698	027	-002	002	005
701	030	011	002	039
723	-050	009	-009	-031
726	-016	-013	000	-030
790	-000	013	003	-033
814	-000	015	019	-007
817	005	006	-010	-014
865	015	013	-001	-006
867	003	021	-015	001
891	035	-015	-028	006
893	016	-020	-030	034
916	035	000	-021	018

Appendix I, continued

Phase		m_λ		
	λ 3330 Å	2980 Å	2460 Å	1920 Å
0.919	0.020	0.013	-0.021	0.017
936	031	034	027	013
942	097	088	011	042
944	082	065	048	071
961	177	184	165	158
967	255	220	214	212
969	269	241	250	247
992	441	421	427	416
0.995	0.453	0.372	0.430	0.437

Note: Heliocentric phases were computed with the ephemeris given in the text for primary minimum.